

Paleoproterozoic low-pressure metamorphism and crustal evolution in the northeastern Yeongnam Massif, Korea

Jeongmin Kim

Korea Basic Science Institute

Abstract

The Yeongnam Massif, one of Precambrian basements in Korean Peninsula, is characterized by widespread occurrence of low-pressure/high-temperature (LP/HT) schists and gneisses accompanying extensive anatexis and granitic magmatism. Metapelitic mineral assemblages define three progressive metamorphic zones pertinent to low-pressure facies series: cordierite, sillimanite and garnet zones with increasing temperature. Metamorphic grade ranges from lower amphibolite to lower granulite facies and metamorphic conditions reach ca. 750 - 800 C and 4 - 6 kbar in migmatitic gneisses. Migmatitic gneisses are prominent in the sillimanite and garnet zones. Textural and petrogenetic relationships in leucosome suggest that migmatitic gneiss is the product of anatexis of metasedimentary rocks. The migmatite formation during the prograde metamorphism is governed initially by fluid-present melting and subsequently by biotite-dehydration melting. The large amount of leucosomes in the sillimanite and garnet zones can be explained by the fluid-present melting possibly triggered by an external supply of aqueous fluid. Field and geochronologic relationships between leucogranites and migmatitic gneisses further suggest that leucogranite has provided fluid and heat required for widespread migmatization.

Introduction

Low-pressure/high-temperature (LP/HT) metamorphic rocks are common in orogenic belts, for example, Variscan fold belt in central Europe (e.g., Will and Schmädicke, 2003), Namaqualand in southern Africa (e.g., Jung et al., 1998), Antarctica (e.g., Johnson et al., 2001) and Cooma Complex in central Australia (e.g., Richards and Collins, 2002). The formation of regional LP/HT metamorphic rocks characterized by andalusite-sillimanite type assemblages requires a transient elevation of the geotherm, exceeding 35 °C/km, in upper and middle sections of continental crust.

The Yeongnam Massif, one of the Precambrian basements in Korean Peninsula, is characterized by widespread occurrences of LP/HT schists and gneisses accompanying extensive anatexis and granitic magmatism. A variety of radiometric age determinations demonstrated that the Yeongnam Massif was primarily evolved from Late Archean and metamorphosed in Early

Proterozoic (Lan et al., 1995; Cheong et al., 2000; Kim and Cho, 2003). However, large uncertainties remain with regard to peak metamorphic condition, pressure-temperature-time (P-T-t) path, and the relationship between metamorphism and granitic magmatism.

In this study, I describe the prograde metamorphism in pelitic to psammopelitic schists and migmatitic gneisses in northeastern Yeongnam Massif. Field relations, reaction textures, mineral chemistries and geothermobarometries were used to constrain the P-T evolution. In addition, systematic progression from the amphibolite to granulite facies in association with the leucogranite production was used for assessing the petrogenetic relationship between high-grade metamorphism and anatectic-melt formation.

Regional geology

The Yeongnam Massif is a polymetamorphic terrain bounded to the north by the Neoproterozoic-Paleozoic Ogcheon Fold Belt, and overlain by ca. 10 km thick Cretaceous sedimentary-volcanic sequences to the southeast (Fig. 1). This massif consists primarily of high-grade gneisses together with minor biotite schist and metapelitic schist. Amphibolites and calc-silicate rocks also occur in subordinate amounts. Metamorphic grade of the Yeongnam Massif ranges from the amphibolite to granulite facies. Episodic granite magmatism and metamorphism is prominent, that is, the earliest crustal formation probably at 2.9 - 2.5 Ga, widespread magmatism at ca. 2.1 Ga, 1.95 Ga and 1.93 - 1.86 Ga, and finally the LP/HT metamorphism at 1.86 Ga (Lan et al., 1995; Cheong et al., 2000; Kim and Cho, 2003).

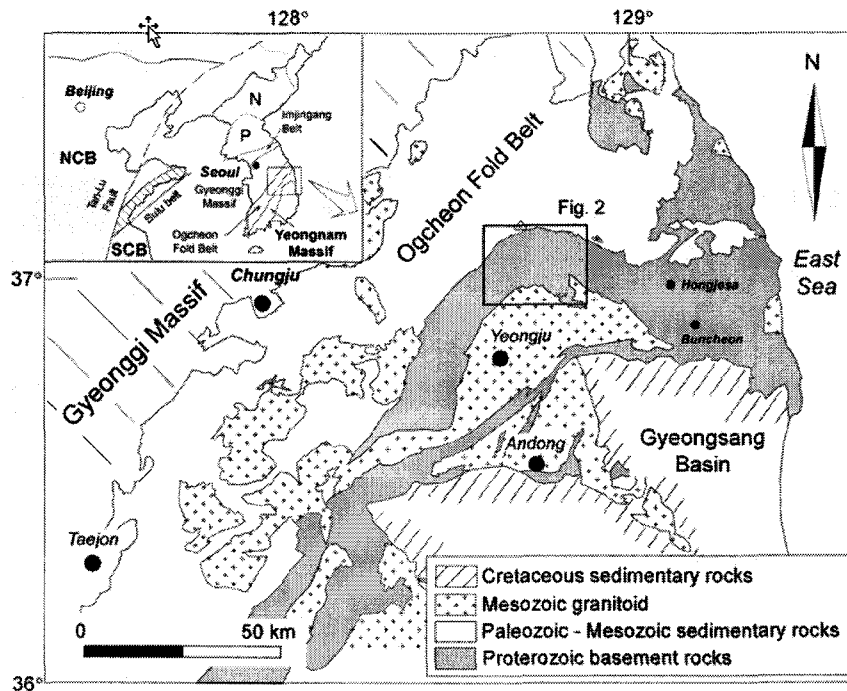


Figure 1. Simplified geologic map of northern Yeongnam Massif (after KIGAM, 1995). The inset figure shows the location of the study area. N: Nangrim Massif, P: Pyeongnam Basin, NCB: North China Block, SCB: South China Block.

The study area, situated in the northeastern part of Yeongnam Massif, mainly comprises two lithologic units of metasedimentary rocks and granitic rocks such as leucogranite and granitic gneiss (Fig. 2). Calc-silicate and mafic rocks rarely occur. Paleozoic sedimentary sequences unconformably overlie the Precambrian basement rocks.

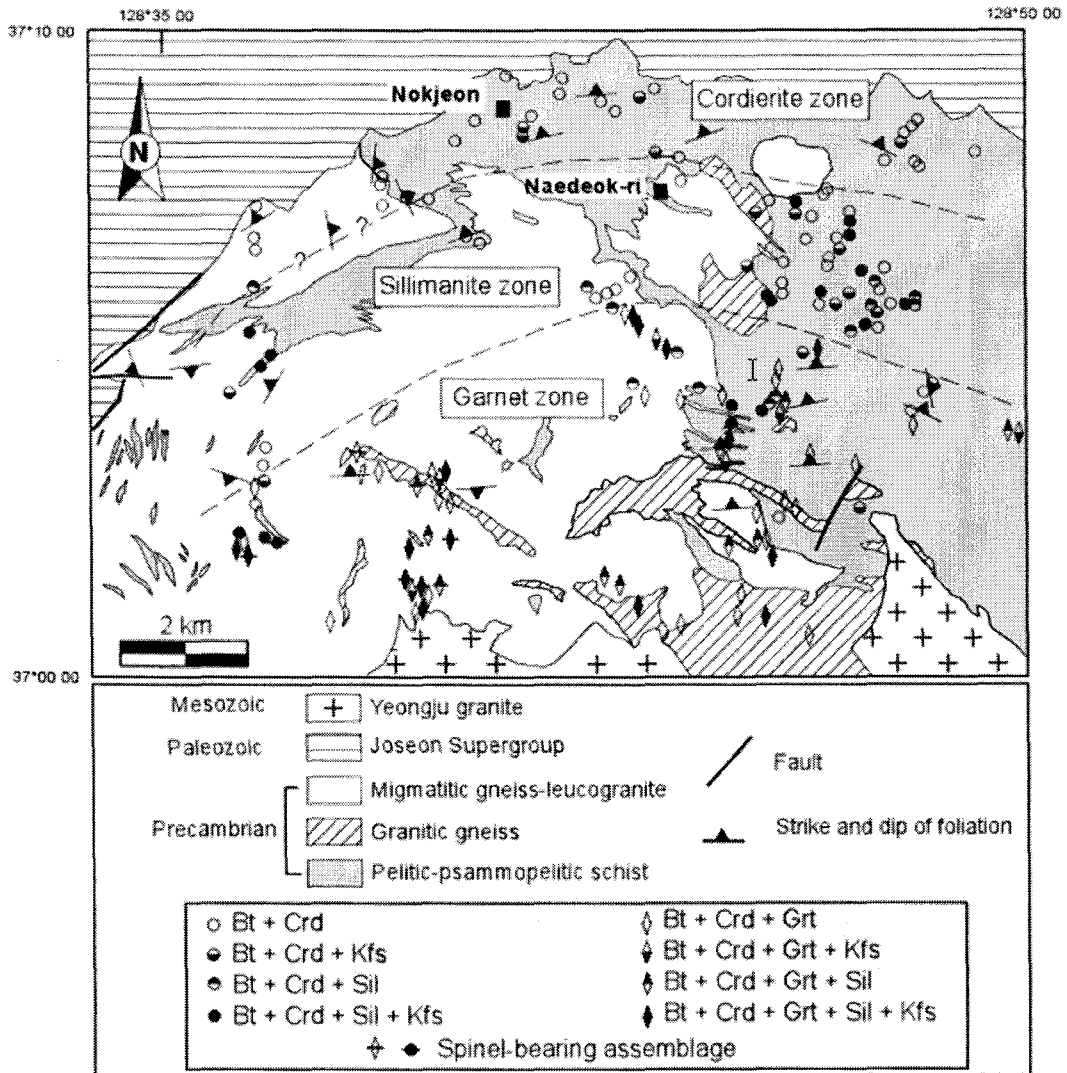


Figure 2. Schematic geologic map of the study area adopted from Lee and Kim (1965) and Lee (1966). Mineral assemblages are also shown for the representative samples of each metamorphic zone. Mineral abbreviations are from Kretz (1983).

Metasedimentary rocks comprise interbedded pelitic and psammopelitic schists or gneisses. Penetrative foliations in metasedimentary rocks are subparallel to lithologic layers, and generally dip towards the north. Metamorphic grade increases southward from lower amphibolite facies to lower granulite facies over a distance of 10 to 15 km. On the basis of mineral assemblages, three metamorphic zones are defined (Fig. 2): the cordierite, sillimanite and garnet zones from

north to south. This progression of metamorphic zones conforms to that of the low-pressure metamorphic terrains (e.g., Morand, 1990; Miyashiro, 1994). In high-temperature zones above the sillimanite-in isograd, pelitic rocks are migmatized, to a variable degree forming metatexite to diatexite. Petrographic characteristics of diatexite are similar to those of leucogranite, except for widespread occurrences of schlieren in the former. The major deformational fabric in study area is the NW-trending foliation in metasedimentary rocks and NNW-trending faults. The oblique crossing of the foliations in metasedimentary rocks and the metamorphic zones suggests that the majority of deformational fabrics observed is not associated with the high-grade metamorphism but rather with the exhumation.

The distribution of each metamorphic zone is broadly concordant with the intrusive boundary of the Yeongju granite. The K-Ar and $^{40}\text{Ar}/^{39}\text{Ar}$ ages of muscovite samples separated from leucogranite and migmatitic gneiss systematically increases from 166 ± 3 Ma to 1383 ± 19 Ma towards the north (Kim, 2004). This result suggests that potential Ar loss in muscovite has occurred during the granite intrusion. Considering the closure temperature for the Ar system in muscovite of ca. 375°C (Spear, 1993), thermal effect of the Yeongju granite seems to be insufficient for disturbing mineral paragenesis and their spatial distributions produced by regional metamorphism.

Garnet-bearing leucogranites intrude as small-scale stocks, sills and subconcordant dykes into pelitic-psammopelitic schists and granitic gneisses. Leucogranites, occurring even in the cordierite zone, are free of any deformation fabric. An extensive network of pegmatitic dykes, up to several meters wide, often develops in association with leucogranites. These pegmatites are undeformed and contain grey K-feldspar, which is characteristic of the Precambrian granitoids in the Yeongnam Massif, including the Hongjesa granitic batholith (Fig. 1). Granitic gneisses occur as small stock-like bodies intruding metasedimentary rocks, and their foliation is generally parallel to that of the country rocks. The preservation of euhedral plagioclase megacrysts suggests an igneous origin for the granitic gneiss. Metamorphic minerals such as garnet, cordierite and/or sillimanite commonly occur in granitic gneiss. Both leucogranite and granitic gneiss often contain abundant xenoliths of metasedimentary rocks. The absence of deformation fabric in leucogranite suggests a deformation event between the intrusions of leucogranite and granitic gneiss.

Petrography

Non-migmatized metasedimentary rocks

Various mineral assemblages of pelitic-psammopelitic schists (Fig. 2) are characterized by the occurrence of cordierite, sillimanite and garnet together with biotite, quartz, plagioclase and K-feldspar. Modal content of each mineral is variable but biotite and cordierite are ubiquitous in all metamorphic zones. Accessory minerals in pelitic to psammopelitic gneisses include

tourmaline, ilmenite, apatite and zircon. Primary muscovite is found only in the northern, lower-grade part of the cordieritezone. The preferred orientation of biotite and fibrolitic sillimanite defines the penetrative schistosity. Cordierite occurs as ubiquitous poikiloblasts ranging up to 2 cm in size. It commonly contains numerous inclusions of quartz and biotite, and aggregates of fibrous or prismatic sillimanite. These inclusions are oriented subparallel to the external foliation. Fibrolitic and prismatic grains of sillimanite are predominant in the sillimanite and garnet zone, respectively. Post-kinematic poikiloblasts of andalusite uncommonly occur in the garnet zone as a product of Jurassic thermal overprint. Together with fine-grained biotite, poikiloblastic andalusite often replaces garnet and cordierite.

Migmatitic gneiss

Stromatic migmatitic gneiss first appears in the sillimanite zone. Patchy or vein-type leucosomes are 3 - 20 mm wide and occur as bedding-parallel layers or boudins in low strain zones. Psammopelitic schists, in contrast to pelitic ones, commonly contain minor amounts of leucosome, reflecting a bulk compositional control on the amount of in-situ melts. The leucosomes consist of medium- to coarse-grained quartz, microcline and plagioclase, together with minor amounts of secondary muscovite and chlorite. Myrmekitic and granophyric intergrowths are common.

Metatextitic migmatites are widespread in the garnet zone, and their leucosomes contain garnet and/or cordierite. Melanosomes consist primarily of medium- to coarse-grained biotite, sillimanite, cordierite, garnet, quartz, spinel and ilmenite. Large garnet porphyroblasts (10 - 20 mm in diameter), containing inclusions of quartz, biotite, sillimanite, cordierite and ilmenite, occur at the interface between leucosome and melanosome. Prismatic sillimanite overgrows garnet and cordierite in the migmatitic gneiss. Fine-grained ilmenite develops along the margin of biotite in melanosomes, reflecting the biotite instability as a result of incongruent melting. Deep-green hercynitic spinel commonly occurs in quartz-absent domains as fine-grained equidimensional inclusions within garnet, sillimanite and cordierite.

Diatextitic migmatites prevail in local domains adjacent to the leucogranite. Quartzofeldspathic diatexites are commonly entrained with biotite-rich schlieren containing polymineralic aggregates of garnet, cordierite, biotite and sillimanite. Mineral assemblages together with the absence of melt-derived textures such as idioblastic crystal faces and graphic intergrowths indicate the restitic origin of schlieren.

Mineral chemistry

Biotite

The compositions of biotite are homogeneous within an individual grain, but vary with

the occurrence and metamorphic grade of the host rock. Biotite occurring as inclusions in garnet has lower X_{Fe} ($=Fe/(Fe+Mg)$) values than the matrix biotite. As metamorphic grade increases from cordierite to sillimanite zones, average X_{Fe} values increase from 0.55 to 0.61. In the garnet zone, the X_{Fe} values are scattered within the range from 0.50 to 0.63. The compositional relationships between the X_{Fe} value and Al^{VI} (octahedral aluminum) content change from negative to positive ones as garnet appears (Fig. 3a). The content of ferromagnesian components, Fe + Mg, is correlated with Al^{VI} (Fig. 3b). Such a linear correlation suggests the substitution of $2Al + \square \rightarrow 3(Fe, Mg)$, where \square denotes octahedral vacancy.

Biotite in the garnet zone is generally higher in Ti contents (average value of 0.16 atoms per formula unit, apfu) than that of the cordierite zone (0.11 apfu). The increase in Ti contents could be attributed to high temperatures of the garnet zone. In the sillimanite zone, biotite shows a positive correlation between the X_{Fe} value and Ti content. This relationship is consistent with that of experimental results on the Fe-Mg biotite (Henry and Guidotti, 2002). However, in the garnet zone, there is no apparent relationship between the X_{Fe} values and Ti concentrations. This scattering is partly related to the re-equilibration or secondary formation of biotite after the regional metamorphism.

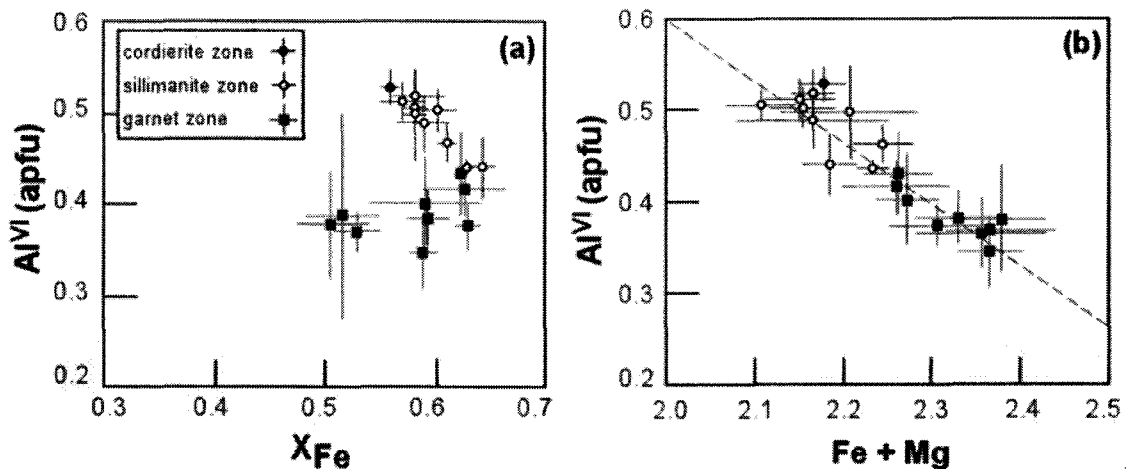


Figure 3. Compositions of biotite from each metamorphic zone. (a) X_{Fe} ($=Fe/(Fe+Mg)$) vs. Al^{VI} and (b) X_{Fe} vs. $Fe + Mg$ calculated on the basis of 11 anhydrous oxygens. Error bars represent the standard deviation (1σ) of compositional range in each sample. The diagonal line in (b) represents the ideal trend of the $2Al + \square \rightarrow 3(Fe, Mg)$ substitution.

Cordierite

The composition of cordierite within single sample is fairly uniform except for slight Fe-enrichment in the core. The X_{Fe} values of cordierite increase from 0.41 - 0.46 in the cordierite and sillimanite zones to 0.45 - 0.50 in the garnet zone. Pereira and Bea (1994) classified cordierites into metamorphic, magmatic and anatectic types, on the basis of variations in the $Mg/(Mg+Fe+Mn)$ value and content of the channel cations comprising Na and K (Fig. 4).

The majority of cordierite belongs to anatectic cordierite shows no remarkable difference in the content of channel cations. Such ambiguities are attributed to the perturbation of channel cations by alteration and/or retrograde metamorphism. However, the cordierite from the garnet zone is plotted in the field of anatectic cordierite.

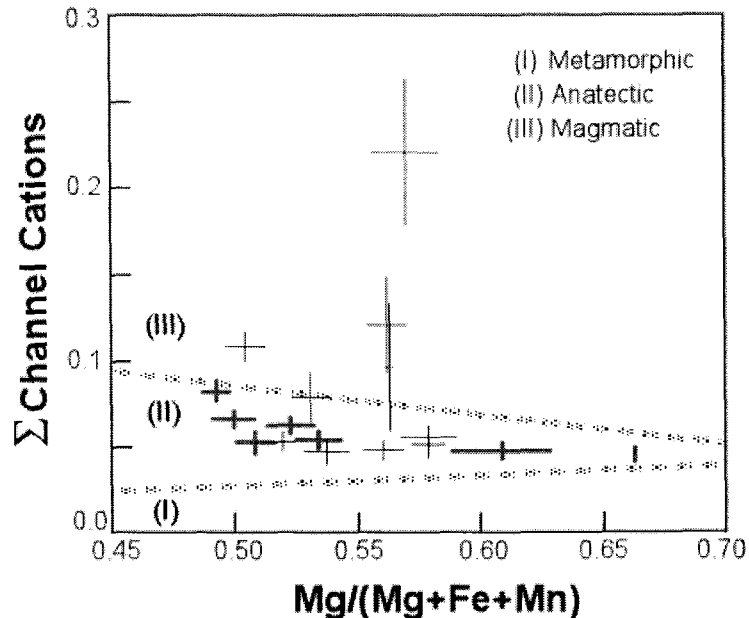


Figure 4. Mg/(Mg+Fe+Mn) vs. sum of channel cations of cordierite in metapelites. Thick cross represents the composition of cordierite from the garnet zone. Error bars represent the 1σ .

Garnet

Garnet porphyroblasts in migmatitic gneisses are rich in the almandine component (77 - 81 mol %), with subordinate amounts of pyrope and spessartine components. The X_{Fe} values of garnet cores range from 0.81 to 0.88. With increasing metamorphic grade, the pyrope contents of garnet cores change from 11 - 13 mol % to 16 - 18 mol %. Most garnet grains show compositional zoning, characterized by increasing X_{Fe} and decreasing pyrope content towards the rim. Slight enrichment of the spessartine content at the outermost rim is the product of diffusional zoning during the retrogression.

Feldspars

K-feldspar is ubiquitous throughout the study area except for the psammitic schist in the cordierite zone. Its orthoclase content, defined as $K/(K+Na+Ca)$, ranges from 76 to 96 mol %, while the anorthite content is less than 1 mol %. No compositional difference is apparent for K-feldspar grains between leucosome and melanosome. Plagioclase in migmatitic gneiss is compositionally homogeneous. The anorthite content (An_{30-31}) of melanosome in migmatitic gneiss is higher than that of leucosome (An_{17-19}).

Spinel

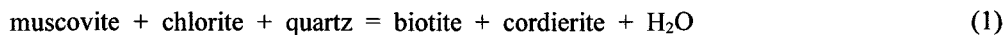
Spinel occurring in the garnet zone is a hercynite-gahnite solid solution. The hercynite component ($=\text{Fe}^{2+}/[\text{Fe}^{2+} + \text{Mg} + \text{Zn}]$) ranges from 0.50 to 0.79, whereas the gahnite component ($=\text{Zn}/[\text{Fe}^{2+} + \text{Mg} + \text{Zn}]$) from 0.11 to 0.39. No compositional zoning is apparent in individual grains.

Mineral paragenesis and reaction relationship

Three metamorphic zones have distinct mineral assemblages and chemistries, resulting from a series of continuous and discontinuous reactions. The sequence of mineral assemblage in each metamorphic zone during prograde metamorphism is shown in Fig. 5. Mineral reactions consisting of cordierite, sillimanite, K-feldspar, garnet, quartz and H₂O (muscovite chlorite) in the KFMASH (K₂O-FeO-MgO-Al₂O₃-SiO₂-H₂O) system were chosen to discuss mineral parageneses observed in the study area. Various P-T grids (e.g., Pattison, 1991; Spear et al., 1999) were used to show univariant reactions and their relative positions in the P-T space. Experimental results for the dehydration melting (Vielzeuf and Montel, 1994; Stevens et al., 1997) were also used for discussing the migmatization observed in the migmatitic gneiss. The majority of the subsolidus curves are adopted from Pattison and Harte (1991), and supersolidus reactions from Powell and Downes (1990), Whittington et al. (1998) and Spear et al. (1999).

Subsolidus reactions

The assemblage of biotite + muscovite + quartz + plagioclase + K-feldspar represents the lowest grade part in the cordierite zone (Fig. 5). Biotite first appears in metapelites at the expense of chlorite and K-feldspar at 420 °C and 3.5 kbar (Bucher and Frey, 2002). The ubiquity of cordierite + biotite in the cordierite zone could be attributed to the following divariant KFMASH reaction:

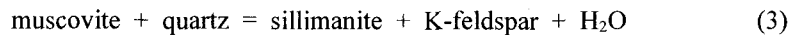


Reaction (1) is known as the lowest-temperature reaction producing the biotite + cordierite assemblage (Xu et al., 1994). According to Pattison and Tracy (1991), this assemblage is stable in pelitic rocks at temperatures higher than ca. 500 °C. Therefore, the temperature condition of the cordierite zone can be in the range of ca. 500-600 °C, which is defined by the reaction (1) and the andalusite = sillimanite equilibrium curve.

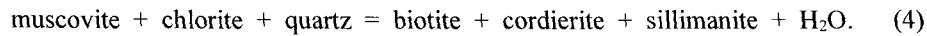
Occurrences of sillimanite in the sillimanite zone can be explained by the following univariant reaction in the KFMASH or KFMASH system and muscovite dehydration reaction with increasing temperature:



and

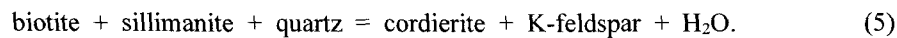


and in the KFMASH system:



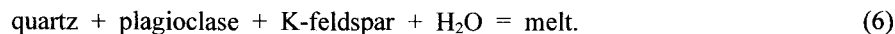
The absence of primary muscovite in the sillimanite zone is presumably attributed to compositional control of the protolith, resulting in complete consumption during the cordierite formation. It is thus difficult to apply reactions (2), (3) and (4) to the sillimanite zone rocks. However, reaction (4) may define the lowest P-T condition for the appearance of sillimanite in the sillimanite zone.

Inclusions of biotite and sillimanite in cordierite are common in the sillimanite zone. This textural relationship suggests the following reaction:



Supersolidus reactions

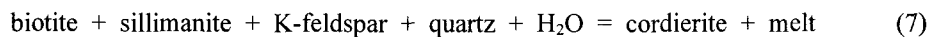
The lack of mafic minerals in leucosome of migmatitic gneisses from the sillimanite zone suggests that the following minimum-melting reaction has occurred:



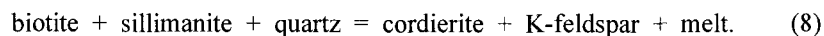
The omnipresence of quartz, K-feldspar and plagioclase in the lower-grade equivalents of migmatitic gneiss of from the garnet zone corroborates the melting by reaction (6).

The dehydration melting reaction of muscovite may form the leucosome without mafic phases at temperatures of ca. 650 C (e.g., Spear et al., 1999). However, as discussed above, the intrinsic small amount of muscovite and subsequent complete consumption during sillimanite forming reaction in the cordierite and sillimanite zones suggests that the muscovite-dehydration melting is not responsible for producing extensive leucosome in migmatitic gneisses.

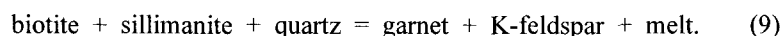
Biotite commonly shows the breakdown texture in the presence of sillimanite. The occurrences of euhedral cordierite in leucosomes as well as the biotite inclusions in cordierite of the garnet zone indicate that cordierite is a peritectic phase produced by the following incongruent melting reactions of biotite:



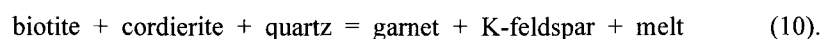
and



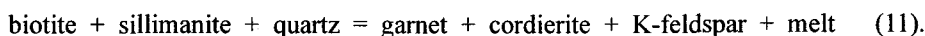
The inclusions such as biotite and sillimanite in garnet in migmatitic gneiss in garnet zone suggest the formation of garnet through the biotite-dehydration melting reaction:



In addition, cordierite occurring as inclusions in garnet suggests that garnet has formed at the expense of cordierite. These textural relations indicate that the following KFMASH reaction is operative:



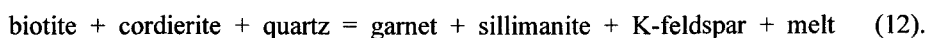
Furthermore, the occurrence of coarse-grained garnet and cordierite in leucosomes suggests that these porphyroblasts are peritectic phases of the biotite-dehydration melting reaction:



Small-grained biotite and sillimanite inclusions in garnet also support reaction (11).

However, the garnet corona on cordierite and the cordierite inclusion in garnet indicate that garnet has formed later than cordierite, possibly by reaction (10).

The prismatic sillimanite replaces the pre-existing cordierite and garnet. The anhedral relics of biotite in the sillimanitemat indicate that sillimanite is the product of biotite-breakdown reaction. This texture suggests that the following reaction is operative at the final stage of migmatization:



The progressive occurrences of peritectic cordierite and garnet in migmatitic gneisses are compatible with experimental results for the dehydration melting at crustal pressures of 5 - 10 kbar (Patino Douce and Johnston, 1991; Vielzeuf and Montel, 1994; Gardien et al., 1995; Stevens et al., 1997). Narrow range of bulk rock X_{Fe} values (0.38 - 0.44) in pelitic to psammopelitic schists and gneisses precludes the possibility that the appearance of garnet results from the change in bulk chemistry.

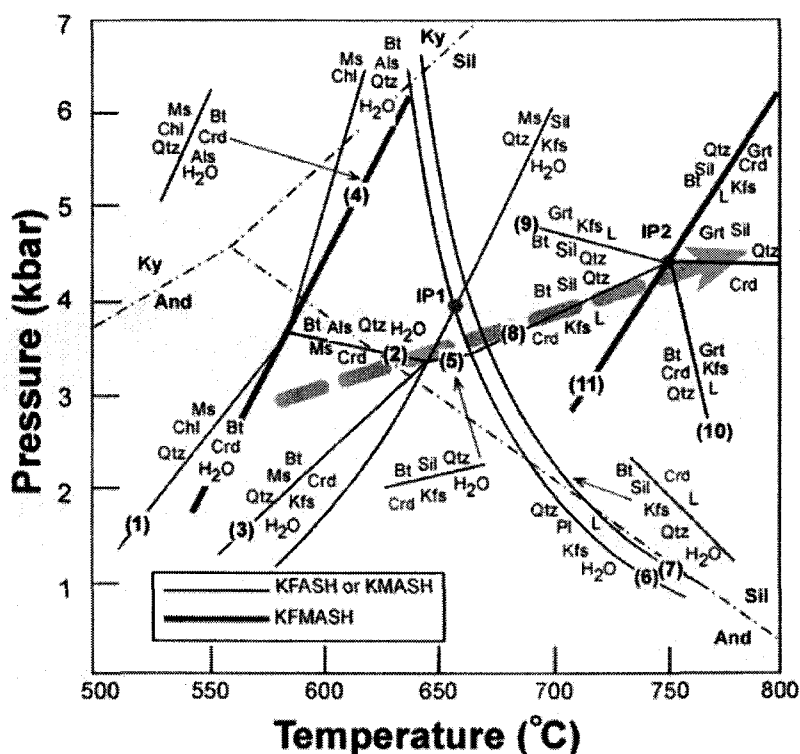
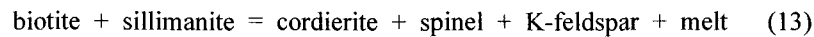


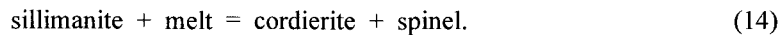
Figure 5. A simplified petrogenetic grid for metapelites in the KFMASH system (after Pattison, 1991). Univariant reactions represent the isopleths of constant $\text{Fe}/(\text{Fe}+\text{Mg})$ values of 0.55 in cordierite. Heavy dashed line approximates the metamorphic field gradient.

Cordierite porphyroblasts in leucosomes are locally replaced by fine-grained, commonly symplectic, aggregates of andalusite, biotite and quartz. This replacement is interpreted to result from the reverse operation of reactions (7) and (8) in the stability field of andalusite. The crystallizing melt could provide aqueous fluid necessary for the retrogression of ferromagnesian minerals such as garnet and cordierite during the cooling. However, extensive preservation of these minerals in leucosomes suggests the loss of anatectic melt from the rock volume and consequently the depletion of excess fluid (e.g., Powell and Downes, 1990; Jung et al., 1998).

Grains of hercynitic spinel commonly coexist with cordierite and occur as inclusions in sillimanite, cordierite and garnet. In addition, the occurrence of spinel is restricted to the quartz-deficient domain. This observation together with the systematic variation in the X_{Fe} values among ferromagnesian phases ($X_{Fe, Spl} > X_{Fe, Bt} > X_{Fe, Crd}$) suggest a prograde reaction:



or a retrograde reaction



The reaction (13) in the KFMASH model system occurs at higher temperatures than reaction (12). However, the introduction of high gahnite component may stabilize spinel at temperatures corresponding to those of Zn-free reaction (12). Therefore, the occurrence of spinel does not necessarily imply an abrupt increase in metamorphic temperatures in the garnet zone.

Metamorphic conditions

P-T condition

Temperature conditions calculated from the garnet-biotite and garnet-cordierite geothermometries range from 530°C to 690°C at an assumed pressure of 5 kbar. Both garnet-plagioclase-biotite-quartz and garnet-plagioclase- Al_2SiO_5 -quartz geobarometers yield the pressure of 4.3 to 6.3 kbar at an assumed temperature of 700°C. The garnet-cordierite-sillimanite-quartz geobarometer also yields similar pressure estimates. Temperatures calculated from geothermometry are incompatible with those defined by phase equilibria governing metamorphic assemblages, whereas pressure estimates are consistent with those from phase equilibria. The discrepancy between phase equilibria and geothermometric calculations is attributed to the resetting of mineral compositions during the cooling stage. Such retrograde effects are prominent in the granulite facies rocks and plutonic igneous rocks which experienced slow cooling.

The average P-T calculations from the THERMOCALC using the assemblage of garnet-cordierite-biotite-sillimanite-K-feldspar-quartz in two samples YJ19 and YJ49-2 from the garnet zone yield the P-T conditions of 600 - 625 °C and 3.8 - 4.1 kbar, and 730 - 748 °C and 4.8 - 5.8 kbar, respectively, assuming the a_{H_2O} value of 0.8 (see below). These two samples represent upper and lower parts of the garnet zone, respectively (Fig. 6). The results of

TWEEQU program are clustered at 705 - 765 C and 4.5 - 6.2 kbar (Kim and Cho, 2003). This result is consistent with that of the THERMOCALC and the GASP and GPBQ pressure estimates.

The peak metamorphic condition can be also constrained by some phase equilibria in the pelitic system. The maximum temperature of the study area is limited by the absence of orthopyroxene-bearing assemblages stable at temperatures above 800 C (Spear, 1993). In addition, the absence of kyanite places an upper pressure limit between 6 and 8 kbar at temperatures of 650 - 750 C. This pressure estimate is compatible with the occurrence of cordierite, because metamorphic cordierite is commonly stable in metapelites at pressures below 6 kbar. In summary, the geothermobarometric calculations and phase equilibria indicate that the peak metamorphic condition of migmatitic gneiss has reached ca. 750 C and 5 - 6 kbar.

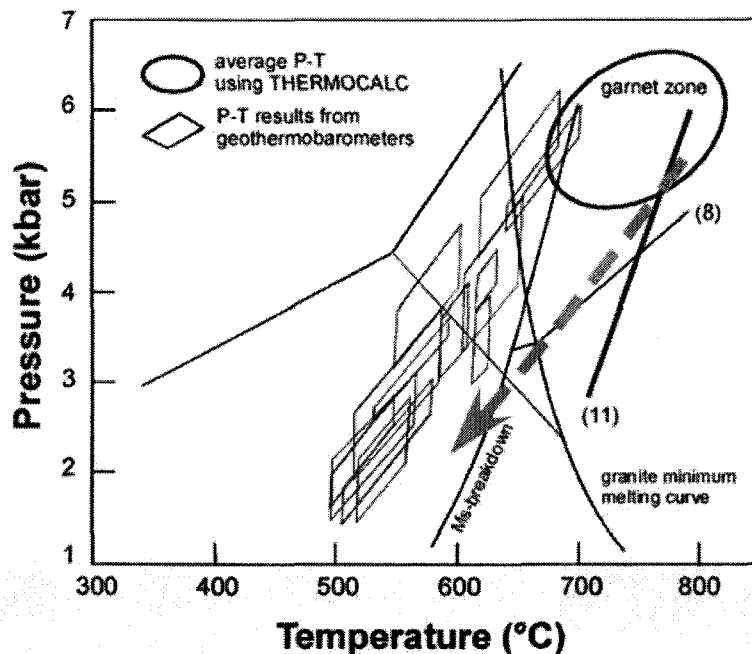


Figure 6. P-T estimates from several geothermobarometers and THERMOCALC calculations. Numbers represent the reaction numbers discussed in text. Thick dashed curve shows the P-T path from garnet zone samples.

Fluid activity during migmatization

The amount of melt during migmatization is strongly dependent on the supply of fluid. According to a recent modeling in the KFMASH system (Johnson et al., 2001), the maximum quantity of melt generated at temperature conditions of the sillimanite zone between reactions (8) and (11) is smaller than 10 % in a fluid-absent condition. In addition, the high $a_{\text{H}_2\text{O}}$ condition is necessary for the generation of cordierite-bearing leucosomes through the infiltration of

external fluid as well as the biotite-dehydration melting. Considering the extent of migmatization and P-T condition in the sillimanite zone, the fluid infiltration is likely to be responsible for the generation of large volume of leucosomes in the sillimanite zone. However, as discussed above section, the phase equilibria in the garnet zone suggest the biotite dehydration reaction was significant. Therefore, at least some part of leucosome was formed by the biotite dehydration reaction. The close field relationship between diatexitic migmatite and leucogranite indicate that the biotite dehydration reaction was significantly responsible for the overall anatexis in the high-grade region in the northeastern Yeongnam massif. Therefore, it is apparent that the migmatization in the study area is governed by both internal and external buffering processes.

During the migmatization, both solid phases and melt should be under identical $a_{\text{H}_2\text{O}}$ conditions. The comparison between P-T values estimated from solid phases and granite solidi for a range of $a_{\text{H}_2\text{O}}$ values can be used to deduce the H_2O activity for the melting reaction (e.g., Whittington et al., 1998). For the migmatitic gneiss (YJ49-2) containing the biotite-garnet-cordierite-spinel assemblage, the minimum $a_{\text{H}_2\text{O}}$ value required for the presence of melt is ca. 0.8 (Fig. 7). The high $a_{\text{H}_2\text{O}}$ value estimated from the garnet zone is compatible with the suggestion of Johnson et al. (2001). If $a_{\text{H}_2\text{O}}$ was much lower than 0.8, the subsolidus assemblage should have been characterized by the coexistence of garnet and cordierite. However, such an assemblage is absent in the garnet zone gneiss.

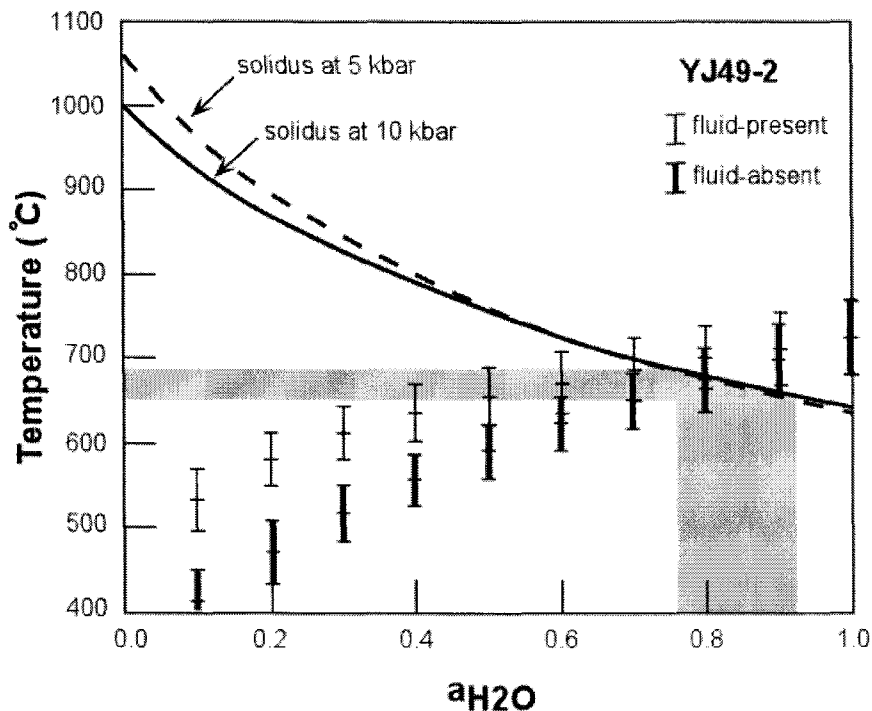


Figure 7. Calculated H_2O activity for the garnet zone samples. Vertical bars represent average temperature calculated using the THERMOCALC at variable of $a_{\text{H}_2\text{O}}$. The shaded portion of solidus curve represents the activity of H_2O during migmatization.

Pressure-temperature history

Metamorphic pressure-temperature (P-T) path was deduced from the progressive metamorphic reactions on the basis of microstructural relationships together with P-T conditions estimated from geothermobarometry. The absence of medium- to high-pressure minerals such as kyanite and staurolite suggests that the prograde metamorphism has accompanied insignificant crustal thickening. Peak metamorphic conditions for the migmatitic gneiss correspond to those of reaction (11) at which the assemblage of biotite + sillimanite + cordierite + garnet + K-feldspar is stable. This reaction defines the transition from the amphibolite to granulite facies in metapelitic rocks (e.g., Bucher and Frey, 2002).

A pseudosection in the KFMASH system constructed for average metapelitic composition by White et al. (2001) was used to reconstruct the P-T path on the basis of the observed mineral assemblage. In the migmatitic gneiss, the inclusions of cordierite and biotite in garnet suggest the transition from the divariant field of cordierite + biotite + K-feldspar + melt to that of garnet + cordierite + biotite + K-feldspar + liquid. On the other hand, prismatic sillimanite replacing garnet and cordierite indicate the transition from the divariant field of garnet + cordierite + biotite + K-feldspar + liquid to that of garnet + sillimanite + cordierite + K-feldspar + liquid. It is thus likely that the prograde P-T path in the migmatitic gneiss is defined by the concomitant increase in both pressure and temperature. However, it is difficult to decipher the retrograde P-T path, because of the absence of any remarkable retrograde product. The exception is the local development of andalusite and chlorite. However, the andalusite is the product of thermal perturbation during the Jurassic granite intrusion. Except for the unconformity between basement rocks and Paleozoic sedimentary rocks, there is no remarkable tectonic movement.

Discussion

The occurrence of peritectic minerals suggest the origin of leucosomes in migmatitic gneisses of the garnet zone as anatectic melts. In addition, the microstructures such as the development of xenomorphic quartz and plagioclase inclusions in euhedral K-feldspar, and the euhedral shapes of garnet and cordierite also support it. This inference is corroborated by the rare connection between leucosomes and adjacent granite bodies (Pattison and Harte, 1991). Moreover, local symplectic intergrowths of biotite and quartz could be attributed to the melt-solid reaction, suggesting the presence of partial melt (Sawyer, 1999).

The different microstructure and mineral assemblages in migmatitic gneiss in sillimanite- and garnet-zones suggest that the two independent partial melting processes are operating in the study area, i.e., biotite-dehydration melting and H₂O-saturated melting. The latter is dominant in the sillimanite zone. The absence of mafic minerals in leucosome indicates that the melting reactions can be modeled by the granite minimum melting. The consumption of muscovite in

the cordierite zone precludes the anatexis through the muscovite-dehydration melting in the sillimanite and garnet zone. Even if any muscovite remains, the coexistence of sillimanite and K-feldspar in the sillimanite zone suggests that muscovite was consumed before the onset of melting. These relations can be explained by the NaKFMASH grid for anatectic migmatites of Spear et al. Initial partial melts forming stromatic migmatites in the sillimanite zone result from the minimum melting. Water-saturated melting near the solidus produces appreciable amounts of melt only if external water is added to the system (Wickham, 1987).

The occurrence of peritectic garnet and cordierite in migmatitic gneiss from the garnet zone suggests a significant role of the biotite dehydration-melting reaction. This observation intimates that the migmatitic gneiss has experienced major melting episode between regions II and III. Incongruent melting reactions of biotite (reactions 7 to 11), which produce a large amount of melt in pelitic rocks (Vielzeuf and Holloway, 1988), occur at 680 - 740 C between 6 and 10 kbar (Le Breton and Thompson, 1988) in common plagioclase-bearing metapelitic rocks. The high modal content of biotite in migmatitic gneisses and the calculated P-T conditions are not compatible with the extensive migmatization through biotite-dehydration melting reaction. As mentioned earlier, high $a_{\text{H}_2\text{O}}$ value implies the ingress of H₂O-rich fluid during the migmatization. It is inferred from the field and geochronologic relations that the migmatization was triggered by the intrusion of leucogranite. The Sm-Nd ages of the leucogranite and the granitic gneiss are identical within error ranges (Kim and Cho, 2003). Thus, the leucogranite is likely to be syn-metamorphic and supplies heat and fluid necessary for the widespread migmatization, especially to the rocks in sillimanite zone. The fluid liberated during the crystallization of leucogranite facilitates the vapor-present melting of metasedimentary gneisses in the sillimanite to form leucosomes in migmatitic gneisses.

The close field relationship between leucogranite and diatexitic migmatite infer the genetic connection between each other. In the eastern margin in YM, the garnet-bearing high-grade gneiss is found only as xenolith or schlieren in garnet-bearing leucogranite. The other metasedimentary rocks had experienced the metamorphism equivalent to the cordierite-zone in study area. Thus, the high-grade metamorphism producing garnet-bearing migmatite is coeval to the formation of leucogranite.

The LP/HT metamorphism is not likely to be the result of the classical crustal thickening metamorphism (e.g., England and Thompson, 1984) alone, but other tectonic processes have to be invoked: e.g., crustal and lithospheric extension (Wickham and Oxburgh, 1985; Sandiford and Powell, 1986), syn-metamorphic magmatic intrusions (e.g., Lux et al., 1986; De Yoreo et al., 1989), crustal thickening associated with lithospheric mantle thinning (Loosveld and Etheridge, 1990), and/or advective heating by infiltrating hot fluids. Given that the leucogranite, dated at ca. 1.86 Ga (Kim and Cho, 2003), occupies approximately 60 - 70 % of the study area, we favor a syn-metamorphic magma intrusion model and regard the pervasive LP/HT metamorphism

as a product of ‘regional contact metamorphism’. It is tempting to relate the magmatism and the associated metamorphism to a subduction-related arc-type setting. On the basis of geochemical data, such a magmatic arc origin of the leucogranite was proposed by Kim and Cho (2003). Kim and Cho (2003) suggested that heat source for the generation of leucogranite is the underplating of the mantle-derived magma and the high content of radiogenic elements in metasedimentary rocks.

However, it is not clear whether the age of metamorphism in cordierite- and sillimanite-zone coincides with that of garnet zone. The further investigation for the U-Pb dating of the zircon and monazite is indispensable to discern the exact age of metamorphism and genetic relationship of the magmatic activity in the Yeongnam Massif.

Conclusions

The pelitic to psammopelitic metasedimentary rocks in the northeastern Yeongnam Massif has the characteristics of the typical low-pressure/high-temperature metamorphism. Progressive metamorphic zones range from cordierite- through sillimanite- to garnet zones. The peak metamorphic condition reaches 750 - 800 °C and 4 - 6 kbar. Combining petrography and phase equilibria, the prograde P-T path is related with a limited thickening during heating. Two stage migmatization such as the fluid-present melting and the biotite-dehydration melting reaction played an important role for the migmatization in the sillimanite and garnet zones. The widespread occurrence of leucogranite and the concomitance between low-pressure metamorphism and the leucogranite intrusion suggest that the leucogranite has supplied the heat and fluid necessary for the migmatization. Further studies are needed to better understand the fluid source and temporal relationships among various thermal events.

References

- Bucher, K., Frey, M., 2002. *Petrogenesis of metamorphic petrology*, Springer-Verlag, Berlin, 318p
- Cheong, C.S., Kwon, S.-T., Park, K.-H., 2000. Pb and Nd isotope constraints on Paleoproterozoic crustal evolution of the northern Yeongnam Massif, South Korea. *Precam. Res.* 102, 207-220.
- De Yoreo, J.J., Lux, D.R., Guidotti, C.V., 1989. The role of crustal anatexis and magma migration in the thermal evolution of regions of thickened continental crust. In: Daly, J.S., Cliff, R.A., Yardley, B.W.D (eds), *Evolution of metamorphic belts*. Geol. Soc. London Special Pub., 43, 187-202.
- England, P., Thompson, A.B., 1984. Pressure-temperature-time paths of regional metamorphism. Part I: Heat transfer during the evolution of regions of thickened continental crust. *Jour. Petrol.*, 25, 894-928.
- Gardien, V., Thompson, A.B., Grujic, D., Ulmer, P., 1995. Experimental melting of biotite + quartz + muscovite assemblages and implication for crustal melting. *Jour. Geophys. Res.*,

- 100, B8, 15581-15591
- Henry, D.J., Guidotti, C.V., 2002. Titanium in biotite from metapelitic rocks: Temperature effects. Crystal-chemical controls, and petrological applications. *Am. Mineral.*, 87, 375-382.
- Johnson, T.E., Hudson, N.F.C., Droop, G.T.R., 2001. Partial melting in the Inzie Head gneisses: the role of water and a petrogenetic gridin KFMASH applicable to anatectic pelitic migmatites. *Jour. Metamorphic Geol.*, 19, 99-118.
- Jung, S., Mezger, K., Masberg, P., Hoffer, E., Hoernes, S., 1998. Petrology of an intrusion-related high-grade migmatite: implications for partial melting of metasedimentary rocks and leucosome-forming processes. *Jour. Meta. Geol.* 16, 425-445.
- Kim, J., Cho, M., 2003. Low-pressure metamorphism and leucogranite magmatism, northeastern Yeongnam Massif, Korea: Implications for Paleoproterozoic crustal evolution. *Precam. Res.*, 122, 235-251.
- Lan, C.-Y., Lee, T., Zhou, X.-H., Kwon, S.-T., 1995. Nd isotopic study of Precambrian basement of South Korea: Evidence for early Archean crust? *Geology* 23, 249-252.
- Le Breton, N., Thompson, A.B., 1988. Fluid-absent (dehydration) melting of biotite in metapelites in the early stages of crustal anatexis. *Contrib. Mineral. Petrol.*, 99, 226-237
- Loosveld, R.J.H., Etheridge, M.A., 1990. A model for low-pressure facies metamorphism during crustal thickening. *Jour. Metamorphic Geol.*, 8, 257-267.
- Lux, D.R., De Yoreo, J.J., Guidotti, C.V., Decker, E.R., 1986. The role of plutonism in low-pressure/high-temperature metamorphic belt formation. *Nature*, 323, 794-797.
- Miyashiro, A., 1994. *Metamorphic petrology*. UCL Press, London, 404 pp.
- Morand, V.J., 1990. Low-pressure regional metamorphism in the Omeo Metamorphic complex, Victoria, Australia. *Jour. Metamorphic Geol.* 8, 1-12.
- Pattison, D.R.M., 1991. P-T-a(H₂O) conditions in the thermal aureole. In: Voll, G., Töpel, J., Pattison, D.R.M. (Eds), *Equilibrium and kinetics in contact metamorphism*. Springer-Verlag, Heidelberg, pp. 327-350.
- Pattison, D.R.M., Harte, B., 1991. Petrography and mineral chemistry of pelites. In: Voll, G., Töpel, J., Pattison, D.R.M. (Eds), *Equilibrium and kinetics in contact metamorphism*. Springer-Verlag, Heidelberg, pp. 135-180.
- Pereira, M.D., Bea, F., 1994. Cordierite-producing reactions in the Pena Negra Complex, Avila batholith, central Spain: the key role of cordierite in low-pressure anatexis. *Can. Min.*, 32, 763-780
- Powell, R., Downes, J., 1990. Garnet-porphyroblast-bearing leucosomes in metapelites: mechanisms, phase diagrams, and an example from Broken Hill, Australia. In: Ashworth, J.R., and Brown, M. (eds.) *High-temperature metamorphism and crustal anatexis*, Unwin Hyman, London, 407p.
- Richards, S.W., Collins, W.J., 2002. The Cooma metamorphic complex, a low-P, high-T (LPHT)

- regional aureole beneath the Murrumbidgee Batholith. *Jour. Metamorphic Geol.*, 20, 119-134.
- Sandiford, M., Powell, R., 1986. Deep crustal metamorphism during continental extension: modern and ancient examples. *Earth Planet. Sci. Lett.*, 79, 151-158
- Sawyer, E.W., 1999. Criteria for the recognition of partial melting. *Phys. Chem. Earth (A)*, 24, 269-279.
- Spear, F.S., Kohn, M.J., Cheney, J.T., 1999. P-T paths from anatectic pelites. *Contrib. Mineral. Petrol.*, 101, 149-164.
- Vielzeuf, D., Holloway, J.R., 1988. Experimental determination of fluid-absent melting relations in the pelitic system. Consequences for crustal differentiation. *Contrib. Mineral. Petrol.*, 98, 257-276,
- Whittington, A., Harris, N., Baker, J., 1998. Low-pressure crustal anatexis: the significance of spinel and cordierite from metapelitic assemblages at Nanga Parbat, northern Pakistan. In: Treloar, P.J., O'Brien, P.J. (Eds.), *What drives metamorphism and metamorphic reactions?* *Geol. Soc. London Spec. Pub.*, pp. 183-198.
- Wickham, S.M., 1987. Crustal anatexis and granite petrogenesis during low-pressure regional metamorphism: The Trois Seigneurs Massif, Pyrenees, France. *Jour. Petrol.*, 28, 127-169.
- Wickham, S.M., Oxburgh, E.R., 1985. Continental rifts as a setting for regional metamorphism. *Nature*, 318, 330-333.
- Will, T.M., Schmädicke, E., 2003. Isobaric cooling and anti-clockwise P-T paths in the Variscan Odenwald Crystalline Complex, Germany. *Jour. Metamorphic Geol.*, 21, 469-480.
- Xu, G., Will, T.M., Powell, R., 1994. A calculated petrogenetic grid for the system $K_2O-FeO-MgO-Al_2O_3-SiO_2-H_2O$, with particular reference to contact-metamorphosed pelites. *Jour. Metamorphic Geol.*, 12, 99-119.